Zeszyty Naukowe Politechniki Częstochowskiej
Budownictwo – Civil Engineering Science
ISSN 0526-5916

Zeszyty Naukowe Politechniki Częstochowskiej nr 31 (2025), 29-35
DOI: 10.17512/znb.2025.1.04

Influence of the secondary emission coefficient on plasma characteristics in an electron gun with inductive excitation

Khrystyna Toiabina[1], Serhii Maikut[2], Olena Gumen[3], Adam Ujma[4]

ABSTRACT:
This study investigates the influence of the secondary electron emission coefficient (γ) on plasma parameters in an electron gun with inductive excitation. A two-dimensional axisymmetric model was developed in COMSOL Multiphysics, incorporating key processes such as electron impact ionization, argon excitation, plasma heating by RF fields, and secondary electron emission. The emission coefficient γ was varied from 0 to 0.2, revealing notable effects on plasma behavior. As γ increased, electron density near the cathode center decreased by approximately 11 %, while the overall ion density grew by about 10 %. Opposite trends were observed in current distributions: the central electron current increased by 11 %, whereas the ion current moderately decreased. A numerical artifact near the symmetry axis was identified and interpreted accordingly. The results confirm the model's physical consistency and its potential as a basis for simulating combined inductive-magnetron systems. Future work will focus on incorporating magnetron excitation to explore interactions between distinct excitation mechanisms and their impact on plasma structure.

KEYWORDS:
induction-magnetron excitation; cold cathode; hybrid plasma systems; optimization of plasma parameters

1. Introduction

Inductively coupled plasma (ICP) is a widely used method for generating dense low-temperature plasma in coating deposition technologies, ion implantation, plasma chemical processing, and vacuum electronics. Due to the absence of electrodes in the excitation region, systems with inductive discharges offer process cleanliness, operational stability, and the ability to independently control both plasma density and ion energy [1-3]. The fundamental physical mechanisms of such discharges – including ionization, excitation, electron drift-diffusion, and Joule heating – have been extensively studied in both experimental and numerical works [4-6].

At the same time, there is growing interest in combining inductive and magnetron excitation as a means of expanding the functional capabilities of plasma sources. Although such hybrid approaches are still insufficiently described in the literature, there is reason to believe they can enable more flexible spatial plasma profile formation or localized excitation enhancement. However, before modeling complex combined systems, it is necessary to develop and verify a reliable model of a "pure" inductive electron gun. This will allow for accurate assessment of the contributions of each mechanism to the discharge behavior.

[1] National Technical University of Ukraine "Igor Sikorsky Kyiv Polytechnic Institute", Beresteiskyi ave, 37, 03056 Kyiv, Ukraine, e-mail: mso089961-eds@lll.kpi.ua, orcid id: 0000-0002-0913-4190
[2] National Technical University of Ukraine "Igor Sikorsky Kyiv Polytechnic Institute", Beresteiskyi ave, 37, 03056 Kyiv, Ukraine, e-mail: toiabina.khrystyna@lll.kpi.ua, orcid id: 0000-0002-0913-4190
[3] National Technical University of Ukraine "Igor Sikorsky Kyiv Polytechnic Institute", Beresteiskyi ave, 37, 03056 Kyiv, Ukraine, e-mail: gumens@ukr.net, orcid id: 0000-0003-3992-895X
[4] University of Applied Sciences in Nysa, ul. Armii Krajowej 7, 48-300 Nysa, Poland, e-mail: adam.ujma@pans.nysa.pl, orcid id: 0000-0001-5331-6808

To this end, a two-dimensional axisymmetric model of an electron gun with inductive plasma excitation was developed in the COMSOL Multiphysics environment. The model incorporates key physical processes: electron impact ionization; stepwise ionization; argon excitation; charge carrier drift-diffusion; plasma heating by high-frequency fields; and secondary electron emission. Particular attention is given to the influence of the secondary emission coefficient γ on the spatial distribution of electron and ion densities, as well as on the cathode's current characteristics.

The resulting model represents the first stage in a series of studies aimed at modeling a combined inductive-magnetron system. The presented results enable validation of individual physical processes and form a foundation for further integration of fields of different nature within a unified numerical physico-topological model.

2. Modeling methodology

Within this study, a two-dimensional axially symmetric model of an electron gun with inductive plasma excitation was developed in the COMSOL Multiphysics environment using the Plasma and Magnetic Fields physics interfaces (Fig. 1a). The cathode is positioned at the top of the system (radius – 1.5 cm, thickness – 2 mm) (Fig. 1b).

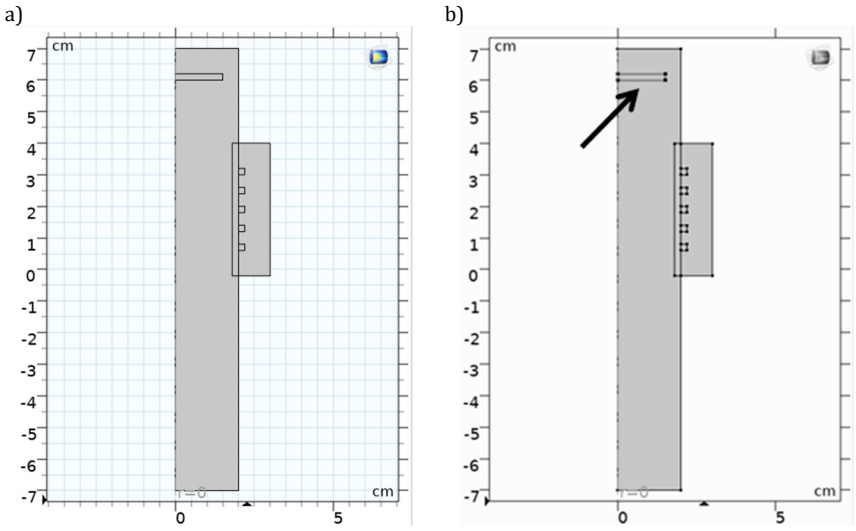

Fig. 1. System geometry: a) general view, b) with the cathode region highlighted

The model was implemented as an axisymmetric cross-section with the following dimensions: system length – 14 cm; radius – 2 cm. The cathode is positioned at the top of the system (radius – 1.5 cm, thickness – 2 mm). The inductor is modeled as five square turns with 2 mm side length, located 2 cm from the axis of symmetry.

The pressure in the chamber was 0.02 Torr (2.664 Pa), and the gas temperature was 300 K. Argon was chosen as the working gas; its volumetric plasma-chemical reactions are listed in Table 1, where Ar denotes argon atoms, Ar^+ – argon ions, and Ar* – metastable argon.

Surface reactions defined in the model are listed in Table 2.

When metastable and ionized argon species reach the chamber walls, they are converted back into neutral atoms. Inductive excitation is implemented by applying an alternating current to the coil at a frequency of 13.56 MHz and a power of 1500 W. Copper is used as the coil material, with an electrical conductivity of $\sigma = 6 \times 10^7$ S/m.

Table 1
Volumetric reactions in argon

No reaction	Formula	Type	Energy [eV]
1	e+Ar => e+Ar	Elastic	0
2	e+Ar => e+Ars	Excitation	11.5
3	e+Ars => e+Ar	Superelastic	–11.5
4	e+Ar => 2e+Ar+	Ionization	15.8
5	e+Ar => 2e+Ar+	Ionization	4.24
6	Ars+Ars => e+Ar+Ar+	Penning ionization	–
7	Ars+Ar => Ar+Ar	Metastable quenching	–

Table 2
Surface reactions defined in the model

No reaction	Type	Sticking coefficient
1	Ar+ => Ar	1
2	Ar+ => Ar	1
3	Ars => Ar	1

The following boundary conditions are set in the model:
- Cathode potential $V = 0$ (grounded);
- Magnetic insulation on the outer boundaries ($n \times A = 0$);
- Dielectric surfaces with dynamic surface charge accumulation ($(\partial\sigma_s/\partial t = n\cdot(J_i + J_e)$).

The obtained equation for the normal component of the electron flux on the wall is defined as:

$$n * \Gamma_e = \frac{1 - r_e}{1 + r_e}\left(\frac{1}{2} v_{e,th} n_e\right) - \left(\sum \gamma_j (\Gamma_j * n) + \Gamma_t * n\right)$$

and for the normal component of the electron energy density:

$$n * \Gamma_\varepsilon = \frac{1 - r_e}{1 + r_e}\left(\frac{5}{6} v_{e,th} n_\varepsilon\right) - \left(\sum \gamma_j \bar{\varepsilon}_j (\Gamma_j * n) + \bar{\varepsilon}_t \Gamma_t * n\right)$$

where:
r_e – the reflection coefficient (usually 0);
$v_{e,th}$ – the thermal velocity (SI unit: m/s);
γ_j – the secondary emission coefficient from the j-th positive ion species;
Γ_j – the ion flux of the j-th positive ion species at the wall (SI unit: $1/(m^2 \cdot s)$);
Γ_t – the thermal emission flux (SI unit: $1/(m^2 \cdot s)$);
ε_j – the mean energy of the j-th species of secondary electrons (SI unit: V);
ε_t – the mean energy of thermally emitted electrons (SI unit: V);
n – the outward normal.

Secondary emission was defined at the cathode with a variable emission coefficient γ, varied parametrically in the range from 0 to 0.2 with a step of 0.05.

The computational mesh was constructed using local refinement in critical regions – near the cathode, the coil, and the discharge zone (Fig. 2).

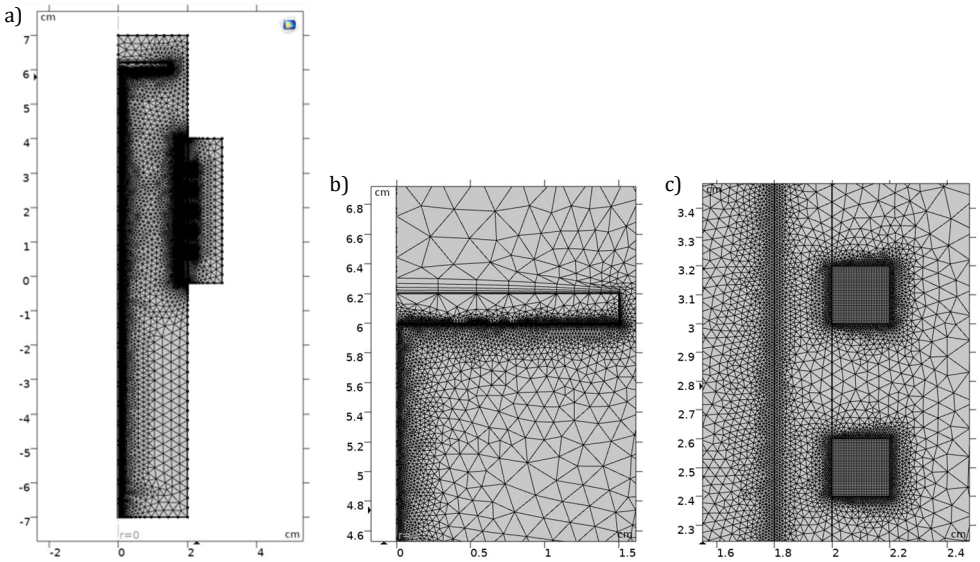

Fig. 2. Calculation grid in the model: a) general view, b) local condensation near the cathode, c) local condensation near the inductor turns

3. Results and discussion

The simulation revealed a strong sensitivity of plasma parameters to the secondary electron emission coefficient γ. In particular, as γ increased from 0 to 0.2, the electron density near the center of the cathode decreased by approximately 11 % – from 1.09×10^{16} m^{-3} to 9.09×10^{15} m^{-3} (Fig. 3a). This effect is attributed to enhanced electron losses due to wall interactions, leading to changes in the local electric field.

At the same time, the electron density along the entire cathode showed a gradual increase of approximately 15 %: from 9.63×10^{15} m^{-3} at $\gamma = 0$ to 1.16×10^{16} m^{-3} at $\gamma = 0.2$. While the overall spatial distribution remained largely unchanged, the plots in Figure 3b, c showed that the minimum electron density in the system increased with higher γ values. This behavior may be associated with the additional contribution of secondary electrons to ionization processes, especially in peripheral regions.

Figure 4 shows the corresponding variation in the ion (Ar^+) density. Throughout the discharge volume, the ion density increases by approximately 10 % – from 7.4×10^{15} m^{-3} at $\gamma = 0$ to 8.15×10^{15} m^{-3} at $\gamma = 0.2$ – without significant changes in the distribution shape. This indicates the enhancement of ionization processes due to the presence of secondary electrons, particularly in the peripheral areas where they tend to accumulate.

A narrow peak in ion density is observed near the geometric center of the cathode ($r = 0$) in Figure 4. This feature is characteristic of axisymmetric models in cylindrical coordinates. In COMSOL Multiphysics, the symmetry axis ($r = 0$) has zero area, but any processes described by equations involving unit area in the denominator (e.g., current or flux) may yield locally overestimated values due to numerical approximation artifacts. Considering the model symmetry and discharge behavior elsewhere, this peak is interpreted as a numerical artifact rather than a physically meaningful ionization enhancement.

Analysis of current distributions on the cathode (Fig. 5) revealed opposite trends in ion and electron currents along the radial direction. The ion current (Fig. 5a) exhibited a moderate decrease with increasing γ across most of the cathode. For instance, in the 0.3 cm - 1.2 cm range, current density decreased by approximately 2 % – 4 %. In the central zone ($r \approx 0$), the peak ion current decreased from 2015 A/m^2 to 1940 A/m^2. However, due to the presence of the numerical

artifact in the ion density distribution near the symmetry axis, these values should be interpreted with caution and are not used for quantitative analysis. At the cathode periphery ($r \approx 1.4$ cm), ion current variations did not exceed 0.2 % – from 2026 A/m² to 2022 A/m².

a)

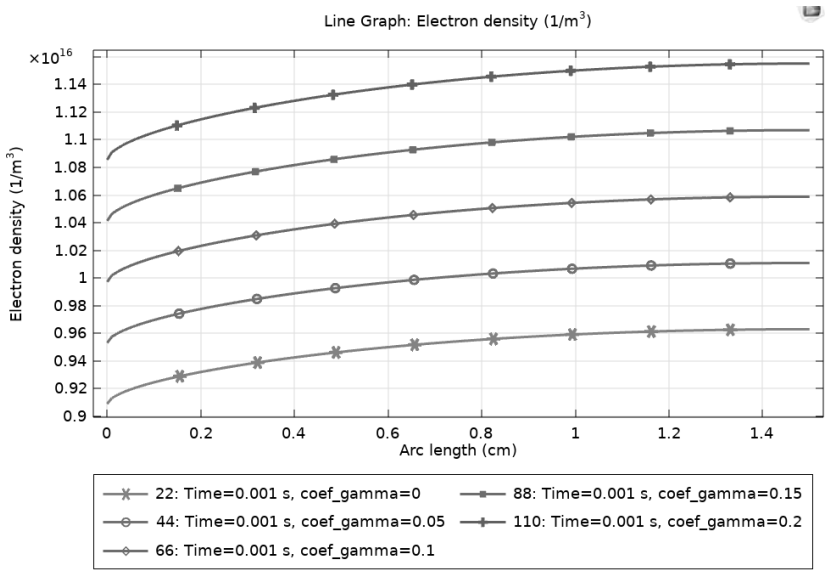

b)

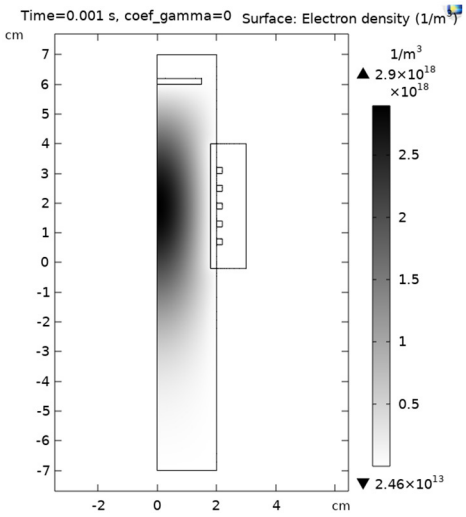

c)

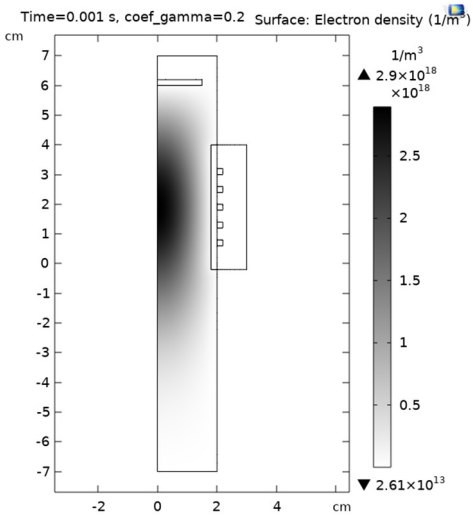

Fig. 3. Electron density: a) at the cathode, from the center to the periphery, b) spatial distribution at $\gamma = 0$, c) spatial distribution at $\gamma = 0.2$

In contrast, the electron current (Fig. 5b) showed an opposite trend: in the center of the cathode, it increased from 1800 A/m² to 2000 A/m² (~11 %), likely due to the return of secondary electrons to the central plasma zone. At the periphery, however, the electron current decreased from 720 A/m² to 480 A/m² (~33 %), which may indicate changes in the geometry of electric field lines and local shielding effects.

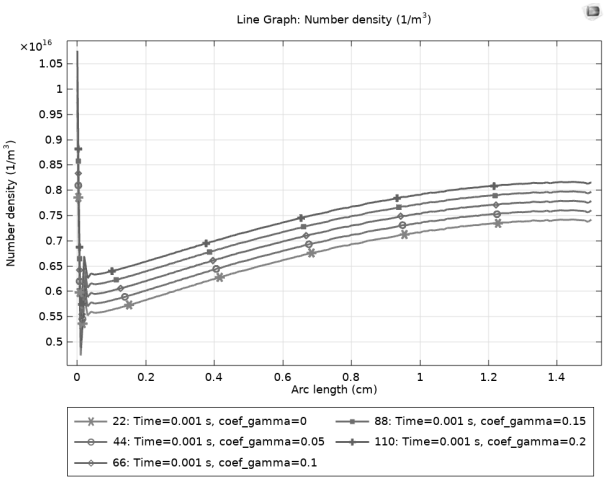

Fig. 4. Ion distribution density at the cathode

a)

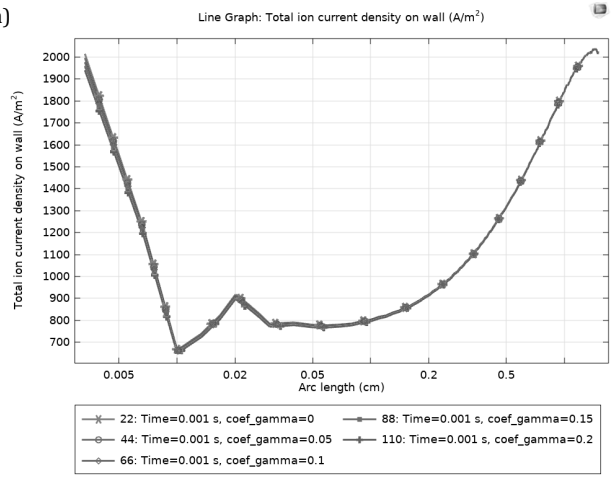

b)

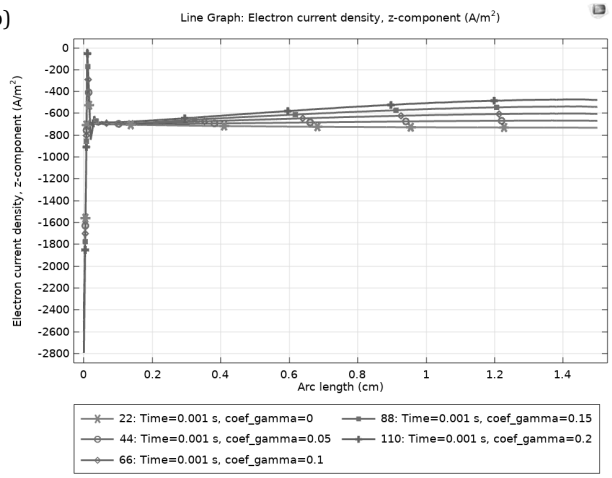

Fig. 5. Current distribution at the cathode: a) ionic, b) electronic

4. Conclusion

The numerical study confirmed that the secondary electron emission coefficient (γ) significantly influences the discharge characteristics. As γ increased from 0 to 0.2, notable changes in plasma behavior were observed: electron density in the central region of the discharge decreased by approximately 11 %, while ion density increased by around 10 % throughout the volume. At the cathode surface, electron current density increased in the central area, whereas ion current density moderately decreased. Variations in the peripheral discharge zone were negligible. A localized ion density peak at the cathode center is interpreted as a numerical artifact of the model and is not considered a physically meaningful effect.

These results confirm the physical validity and numerical reliability of the model, establishing a solid foundation for future development. The next phase of research will focus on incorporating magnetron excitation, enabling the simulation of a combined system to study interactions between electric and magnetic fields and achieve more precise control over the spatial distribution of plasma.

Importantly, the proposed modeling approach offers promising opportunities for the development and optimization of advanced materials, particularly in the construction industry, where plasma-assisted processes can be used to tailor surface properties, enhance durability, and improve the performance of structural components. By enabling detailed control and prediction of plasma-material interactions, these methods can accelerate the design of innovative materials with improved mechanical, thermal, or chemical resistance tailored to modern construction needs.

References

[1] Park S.J., Min C.K., Park Y.G., Jang S.D., Jang G.Y., Shin H.S., Design improvements of electron gun for PAL klystron, Journal of the Korean Physical Society 2025, DOI: 10.1007/s40042-025-01338-1.

[2] Tranquille G., Cenede J., Welker E.S., Galante B., (2024), JACOW: Development of a Field Emission Electron Gun for Low Energy Electron Cooling. JACoW COOL, 2023, THPOSRP10.

[3] Yi Z., Xu Y., Zhang J., Simulation design of an electron gun for microchannel plate scrubbing, Electronics 2025, 14(3), 614, DOI: 10.3390/electronics14030614.

[4] Wei X., Mitchell A., Sun R., Yu N., Yamamura K., A review of simulation modeling of the state evaluation and process prediction of plasma processing under atmospheric pressure, Nanomanufacturing and Metrology 2024, 7(1), DOI: 10.1007/s41871-024-00234-9.

[5] Jia C., Linhong J., Yu Z., Yixiang S., Fluid model of inductively coupled plasma etcher based on COMSOL, Journal of Semiconductors 2010, 31(3), 032004, DOI: 10.1088/1674-4926/31/3/032004.

[6] Bouherine K., Leroy O., Numerical investigation of characteristics and excitation effects on discharge properties in an inductively coupled plasma torch, AIP Advances 2023, 13(4), 045015, DOI: 10.1063/5.0139959.

Wpływ współczynnika emisji wtórnej na charakterystykę plazmy wzbudzanej indukcyjnie przez działo elektronowe

STRESZCZENIE:
Zbadano wpływ współczynnika emisji wtórnej elektronów (γ) na parametry plazmy wzbudzanej indukcyjnie przez działo elektronowe. W projekcie COMSOL Multiphysics opracowano dwuwymiarowy model osiowo-symetryczny, obejmujący kluczowe procesy, takie jak jonizacja uderzeniowa elektronów, wzbudzenie argonem, ogrzewanie plazmy przez pole RF i wtórna emisja elektronów. Współczynnik emisji γ wahał się od 0 do 0,2, wykazując znaczący wpływ na zachowanie plazmy. Wraz ze wzrostem γ gęstość elektronów w pobliżu środka katody zmniejszyła się o około 11 %, podczas gdy ogólna gęstość jonów wzrosła o około 10 %. W rozkładzie prądów zaobserwowano odwrotne tendencje: prąd elektronów w centrum wzrósł o 11 %, podczas gdy prąd jonowy umiarkowanie zmalał. Został zidentyfikowany i odpowiednio zinterpretowany wynik obliczeń numerycznych dla obszaru w pobliżu osi symetrii. Wyniki potwierdzają fizyczną spójność modelu i jego potencjał jako podstawy do symulacji połączonych układów indukcyjno-magnetronowych. Przyszłe badania będą koncentrowały się na wykorzystaniu wzbudzenia magnetronowego do zbadania interakcji między różnymi mechanizmami wzbudzenia i ich wpływu na strukturę plazmy.

SŁOWA KLUCZOWE:
wzbudzenie indukcyjno-magnetronowe; zimna katoda; hybrydowe układy plazmowe; optymalizacja parametrów plazmy